Note: This was previously an Invited Paper presented to the
XVI ENCUENTRO DEL GRUPO ESPAÑOL DE FRACTURA
Torremolinos, Spain, 14-16 April 1999

VIBRATION FATIGUE ANALYSIS IN THE FINITE ELEMENT ENVIRONMENT

NWM Bishop

MSC.Software Limited, Lyon Way, Frimley, Camberley, Surrey, UK

ABSTRACT

Fatigue damage is traditionally determined from time signals of loading, usually in the form of stress or strain. However, there are many design scenarios when the loading, or fatigue damage process, cannot easily be defined using time signals. In these cases the design engineer usually has to use a test based approach to evaluate the fatigue life of his structure or component. Or, alternatively, a frequency based fatigue calculation can be utilised where the loading and response are represented using Power Spectral Density (PSD) functions. One very important design problem, which falls into this category, is that of acoustic fatigue. However, there are also many other situations where structures are subjected to a random form of loading such as wing flutter, landing gear runway profiles, engine vibrations and so on. All of these situations can be analysed using new fatigue life estimation techniques now incorporated into the Finite Element Analysis (FEA) environment.

The theory of random vibration fatigue has seen a number of important developments over the last fifteen years. The author has been personally involved in developing new fatigue analysis theories and structural analysis techniques in the frequency domain (see [1]-[9]). More recently this work has focused on the link with FEA because of the powerful design opportunities which this creates. The work has found many important practical applications. This paper presents a state of the art perspective of random vibration fatigue technology and FEA based fatigue analysis. A number of design applications are presented.

1. INTRODUCTION

Finite Element based tools for fatigue life prediction are now widely available (see for instance [1]). The basic aim of such tools is to enable fatigue life calculations to be done at the design stage of a development process. Imagine being able to check the fatigue life of the engine FEA model shown in Figure 1 long before a prototype exists.

A very important part of these new FEA based tools is a vibration fatigue capability and this paper provides a state of the art review of this technology. It is necessary to clarify the term ***vibration fatigue*** as the estimation of fatigue life when the stress or strain histories obtained from the structure, or component, are random in nature and therefore best specified using statistical information about the process. The same approach can also be described using the terms ***spectral fatigue analysis***, or ***frequency based fatigue*** techniques.

Nearly all structures or components have traditionally been designed using time based structural and fatigue analysis methods. However, by developing a frequency based fatigue analysis approach, the true composition of the random stress or strain responses can be retained within a much optimised fatigue design process. This can yield many advantages, the most important being, (i) an improved understanding of system behaviour, (ii) the capability to fully include the true structural behaviour rather than a potentially inadequate simplified version and (iii) a more computationally efficient fatigue analysis procedure.

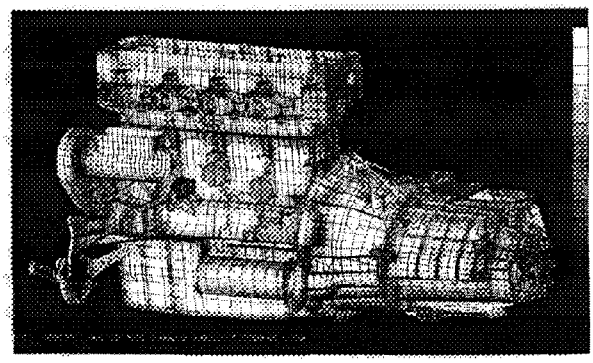

Figure 1. Goal - to 'design' for fatigue

2. ALTERNATIVE DESCRIPTIONS OF ENGINEERING PROCESSES

Most designers, if asked to specify a random loading input, or response output, for a structural system would specify the random time history shown in Figure 2. This process can be described as ***random*** and in the ***time domain***.

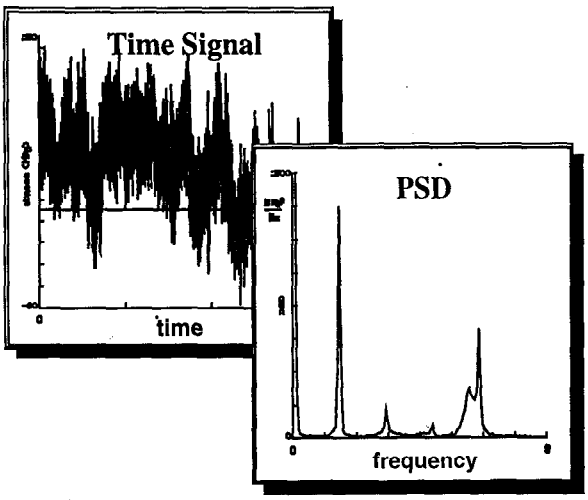

Figure 2. Random processes

The process is described as random because, strictly speaking, it can only be determined statistically. A second sample taken for the same process would obviously have different values to the first.

There are several alternative ways of specifying the same random process. Fourier analysis allows any random loading history of finite length to be represented using a set of sine wave functions, each having a unique set of values for amplitude, frequency and phase. Such a representation is called ***deterministic*** (Figure 3) because the individual sine waves can be determined precisely at any given point in time.

It is still time based and so is therefore specified in the time domain. As an extension of Fourier analysis, Fourier transforms allow any process to be represented using a spectral formulation such as a PSD function. Such a process is described as a function of frequency and is therefore said to be in the ***frequency domain*** (see Figure 2). It is still a random specification of the function.

For the vast majority of engineering problems, if you have one form of the above three loading specifications you can quite easily get to one of the two alternative specifications. These transformations rely on the assumption that the process is stationary, random and Gaussian (see later). Fortunately, most engineering processes conform reasonably well to these assumptions.

Analysis Options

Coupled with each of these three specifications for the loading are three alternative analysis types. The key question for a designer is therefore which type of structural analysis to use, and subsequently which type of fatigue analysis approach to use (see Table 1). For instance, the environmental conditions experienced by aircraft structures can be represented using either a discrete (deterministic) gust approach, or a continuous gust spectrum of atmospheric turbulence.

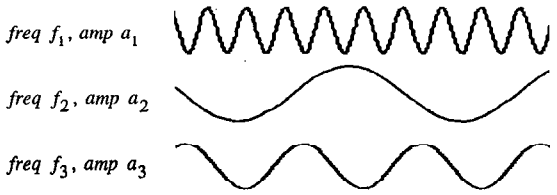

Figure 3. Deterministic processes

When using a discrete gust approach the gust has to be tuned to the natural frequency of the structure in order to avoid a non-conservative result. In contrast, because the gust spectrum is a characteristic of the atmospheric loading, the input loading and structural system are de-coupled. This is typical of a random (PSD) type of analysis where a transfer function is used to represent the structural system. Furthermore, the gust spectrum is a more accurate representation of the input loading than the derived discrete gust.

Table 1. Deterministic and random loading specifications for different industries

	AIRCRAFT	AUTOMOTIVE	OFFSHORE STRUCTURES	WIND TURBINES
DETERMINISTIC	*discrete gust (eg 1-cos wave)*	*kerb strike*	*design wave (eg Stokes 5th)*	*discrete gust*
RANDOM	*continuous gust spectrum of atmospheric turbulence*	*pave*	*sea state spectrum*	*continuous gust*

Because of these factors it is usually desirable, where possible, to do the structural analysis in the frequency domain using PSD's and transfer functions. However, until recently there was no generally applicable fatigue tool to complete the analysis and so this has significantly restricted the use of the random PSD approach. Later sections in this paper show that this is no longer true.

What is the frequency domain?

Structural analysis can be carried out in either the time or frequency domains as shown in Figure 4. In the time domain the input takes the form of a time history of load (in this case wind speed). The structural response can be derived using a finite element representation coupled with a transient (convolution) solution approach. The output from this model is also expressed as a time history, in this case the stress at some particular location in the structure.

In the frequency domain the input is given in the form of a PSD of wind speed and the structure is modelled by a linear transfer function relating input wind speed to the output stress at a particular location in the structure. The output from the model is expressed as a PSD; in this case it is the PSD of stress.

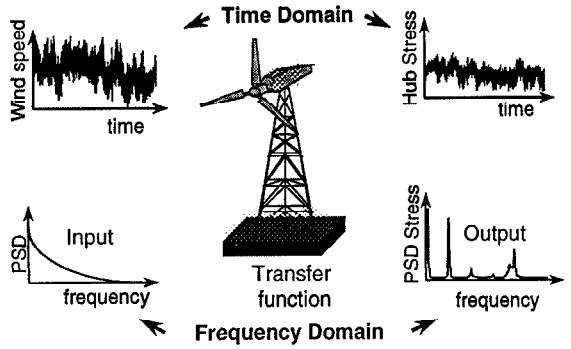

Figure 4. What is the frequency domain?

Most of the computational time is spent in solving the structural model. In the time domain, the structural model is solved for each time history of input; hence 20 load cases would take 20 times as long to calculate as 1. In the frequency domain the linear transfer function is only calculated once, hence 20 load cases takes little more time to analyse than 1. Obviously, if we are calculating a linear structural model then the structure must behave linearly. Fortunately in most engineering situations this is a reasonable assumption.

The Fourier Transform

Basically, the frequency domain is another way of representing a time history. Certain information about a random process becomes apparent in a frequency domain plot, which is difficult to see in the time domain. It is easy to flip back and forth between the two domains using the Fourier Transformation and Inverse Fourier Transformation respectively (Figure 5). In this way an Engineer can see both time and frequency domain representations of a signal in the same way as he would flip a graph between log and linear axes to gain a different perspective.

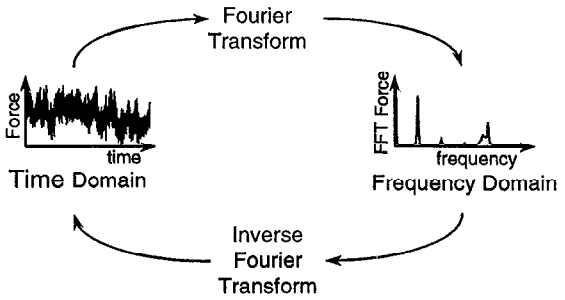

Figure 5. The Fourier Transformation

What does an FFT tell us?

The Fast Fourier Transform (FFT) outputs a complex number given with respect to frequency. A sine wave of frequency w, amplitude *A* and initial phase angle j is represented in the frequency domain by a spike occurring at w along the frequency axis. If the magnitude of the complex FFT is plotted, then the area under the spike is found to be the amplitude *A* of the sine wave. When the argument of the complex FFT is plotted then the area is found to be initial phase angle j of the sine wave. The frequency, amplitude and phase of the sine wave are therefore retained in both the time and frequency domains.

Any periodic function can be expressed as the summation of a number of sinusoidal waves of varying frequency, amplitude and phase (see Figure 6). Each individual sinusoidal wave can be expressed as a spike in the frequency domain and as the number of sine waves increase, the difference in frequencies between them tend to zero and so the spikes tend to merge into a continuous function.

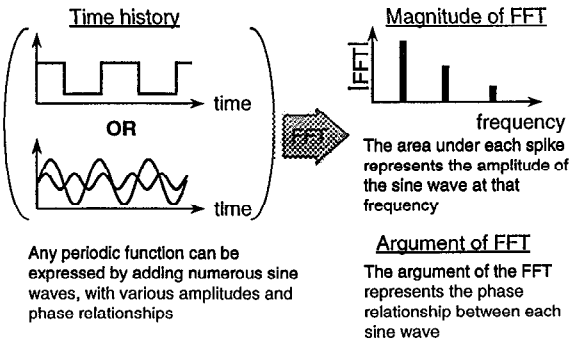

Figure 6. Using an FFT to characterise a time signal

In most engineering situations it is only the amplitude of the various sine waves which is of interest. In fact, in

many cases we find that the initial phase angle is totally random, and so it is unnecessary to show it. For this reason the PSD function alone is usually used.

What is a Power Spectral Density (PSD)?

PSD's are obtained by taking the modulus squared of the FFT (see Figure 7). In a PSD only the amplitude of each sine wave is retained. All phase information is discarded.

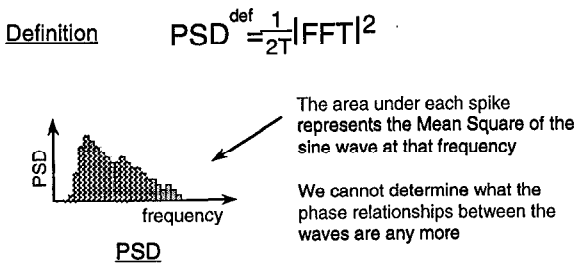

Figure 7. What is a PSD?

Getting a representative time series.

Many design standards give data on random processes in the form of PSD's. This is particularly true of environmental conditions such as wave surface profiles, wind speeds and earthquake accelerations. A PSD contains no information about phase relationships between the individual sine waves and without this a time series cannot be recreated. For processes which are Gaussian, stationary and random it has been observed that the phase angles are randomly distributed. This observation allows a representative time series to be created which is statistically similar to the original.

Figure 8 gives an engineering perspective of how this might be done. Firstly, if the PSD is split into, say, 40 strips and the area of each strip found, the area of each strip can be used to produce an equivalent sine wave by taking the square root of the area and multiplying by 1.41. This come from the observation that the rms of a sine wave is equal to its peak height divided by 1.41, and the rms of each strip in the PSD is equal to the square root of its area. In this way an equivalent set of 40 sine waves can be produced. The time history regenerated will not be exactly the same as the original but will be statistically equivalent.

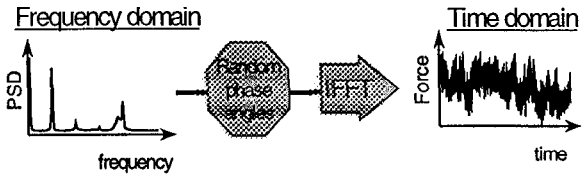

Figure 8. Generating a time series from a PSD

3. CHARACTERIZATION OF ENGINEERING PROCESSES USING STATISTICAL MEASURES

Time histories & PSD's

Engineering processes can fall into a number of types and Figure 9 is useful as a means of characterising these different types of processes. In Figure 9(a), a ***sinusoidal time history*** appears as a single spike on the PSD plot. The spike is centred at the frequency of the sine wave and the area of the spike represents the mean square amplitude of the wave. In theory this spike should be infinitely tall and infinity narrow for a pure sine wave. However, because any sine wave used is, by definition, finite in length, the spike always has finite height and finite width. Remember, with PSD plots it is the area under the graph that is of interest and not the height of the graph.

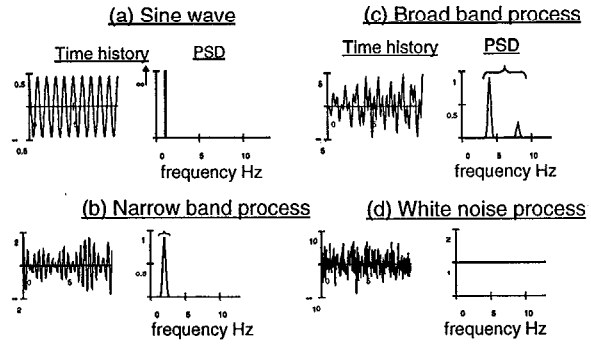

Figure 9. Equivalent time histories and PSD's

In Figure 9(b), a ***narrow band process*** is shown which is built up of sine waves covering only a narrow range of frequencies. A narrow band process is typically recognised in a time history by amplitude modulation, often referred to as a 'beat' envelope.

In Figure 9(c), a ***broad band processes*** is shown which is made up of sine waves over a broad range of frequencies. These are shown in the PSD plot as either a number of separate response peaks (as illustrated) or one wide peak covering many frequencies. This type of process is usually more difficult to identify from the

time history but is typically characterised by positive valleys (troughs in the signal above the mean level) and negative peaks.

In Figure 9(d), a ***white noise process*** is shown. This is a special time history, which is built up of sine waves over the whole frequency range.

Expected zeros, peaks and irregularity factor

Random stress or strain time histories can only properly be described using statistical parameters. This is because any sample time history can only be regarded as one sample from an infinite number of possible samples that could occur for the random process. Each time sample will be different. However, as long as the samples are reasonably long then the statistics of each sample should be constant. Two of the most important statistical parameters are the number of so-called ***zero crossings*** and ***number of peaks*** in the signal. Figure 10 shows a 1 second piece cut out from a typical wide band signal.

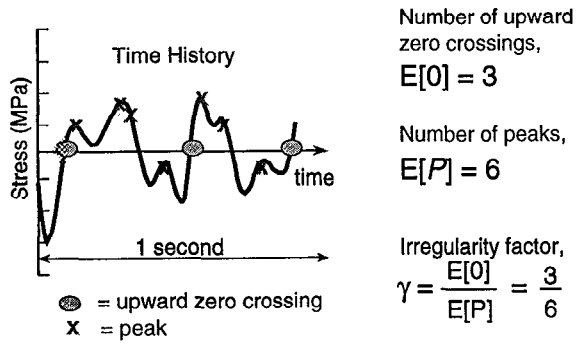

Figure 10. Zero and peak crossing rates

E[0] represents the number of (upward) zero crossings, or mean level crossings for a signal with a non-zero mean. *E[P]* represents the number of peaks in the same sample. These are both specified for a typical 1 second sample. The irregularity factor is defined as the number of upward zero crossings divided by the number of peaks.

In this particular case the number of zeros is 3, and the number of peaks is 6, so the irregularity factor is equal to 0.5. This number can theoretically only fall in the range 0 to 1. For a value of 1 the process must be narrow band as shown in Figure 9(b). As the divergence from narrow band increases then the value for the irregularity factor tends towards 0.

Probability density functions (pdf's)

The most convenient way, mathematically, of storing stress range histogram information is in the form of a ***probability density function (pdf)*** of stress ranges. A typical representation of this function is shown in Figure 11. It is very easy to transform from a stress range histogram to a pdf, or back. The bin widths used, and the total number of cycles recorded in the histogram, are the only additional pieces of information required. To get a pdf from a ***rainflow*** (see later section) histogram each bin in the rainflow count has to be multiplied by $S_t \times dS$ where,

S_t = total number of cycles in histogram

dS = interval width

The probability of the stress range occurring between

$$S_i - \frac{dS}{2} \text{ and } S_i + \frac{dS}{2} \text{ is given by } p(S_i)dS \qquad (1)$$

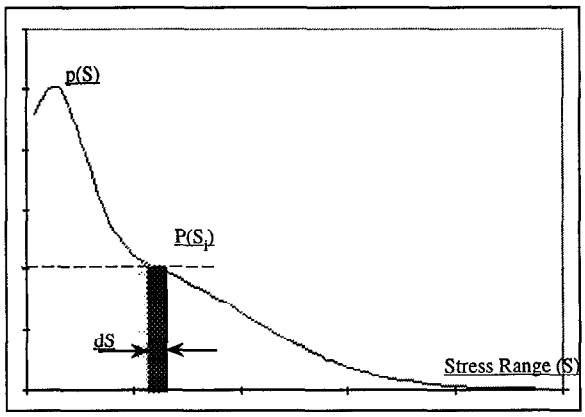

Figure 11. Probability density functions

Moments from a PSD

Since we are concerned with structural systems analysed in the frequency domain a method is required for extracting the pdf of rainflow ranges directly from the PSD of stress. The characteristics of the PSD that are used to obtain this information are the ***nth moments*** of the PSD function (Figure 12). The relevant spectral moments are easily computed from a one sided PSD G(f) in units of Hertz using the following expression.

$$m_n = \int_0^\infty f^n \cdot G(f)df = \sum f_k{}^n \cdot G_k(f) \cdot \delta f \qquad (2)$$

The n^{th} moment of area of the PSD (m_n) is calculated by dividing the curve into small strips as shown. The n^{th} moment of area of the strip is given by the area of the strip multiplied by the frequency raised to the power n. The n^{th} moment of area of the PSD is then found by summing the moments of all the strips.

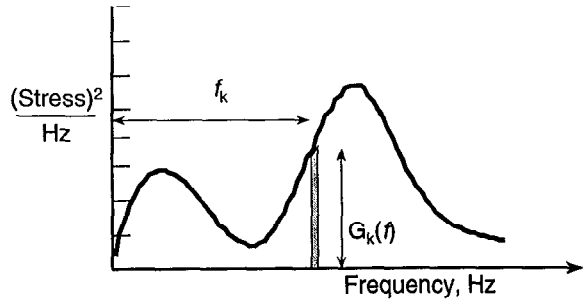

Figure 12. Calculating PSD moments

In theory, all possible moments are required to fully characterise the original process. However, in practice, we find that m_0, m_1, m_2 and m_4 are sufficient to compute all of the information required for the subsequent fatigue analysis.

Expected zeros, peaks and irregularity factor from a PSD.

The first serious effort at providing a solution for estimating fatigue damage from PSD's was undertaken by SO Rice in 1954 [10]. He developed the very important relationships for the number of upward mean crossings per second (E[0]) and peaks per second (E[P]) in a random signal expressed solely in terms of their spectral moments m_n.

$$E[0]=\sqrt{\frac{m_2}{m_0}} \quad E[P]=\sqrt{\frac{m_4}{m_2}} \tag{3}$$

$$\gamma=\frac{E[0]}{E[P]}=\sqrt{\frac{m_2^2}{m_0 m_4}} \tag{4}$$

Pdf of peak position and amplitude.

Two important pdf's can be computed from a stress or strain time history. These are the amplitude and peak pdf's as shown in Figure 13. The best way to visualize these parameters is to draw tram lines horizontally through the time history and then count either the number of times the signal crosses the tram lines or the number of times a peak occurs in-between the tram lines. The complete pdf's are obtained by repeating this process for all horizontal levels in the signal. For most engineering purposes the amplitude pdf will be approximately Gaussian. Furthermore, for a narrow band process the peak pdf will be approximately equivalent to the Rayleigh pdf.

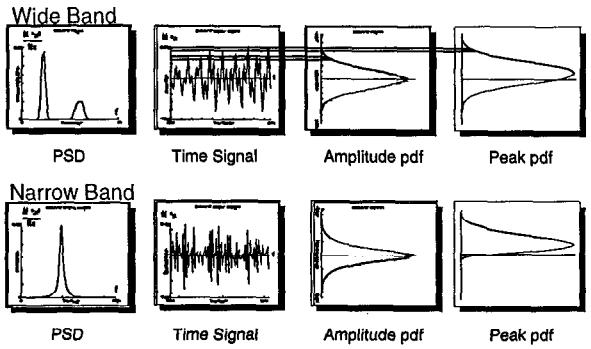

Figure 13. Amplitude and peak pdf's

What is the Transfer Function?

If a sinusoidal force is applied to a linear structure then the structure will respond with a sinusoidal displacement at the same frequency. For a linear structure we can also expect that an increase in the amplitude of the forcing function will cause a proportional increase in the structural displacement. This leads to the concept of a linear ***transfer function.***

The transfer function is defined as the response per unit input at each frequency of interest as shown Figure 14. We can therefore use the transfer function to predict the amplitude displacement of the structure by multiplying the amplitude of the load F by the transfer function T for a particular frequency of applied load.

The transfer function can be calculated using a number of methods. These include computer generated models (FEA analysis) and using data acquired from tests. An intuitive way to calculate it would be to apply a series of sine waves to a test rig, or an FEA model, and then find the amplitude of the structural response for each frequency. The structural response doesn't have to be in the form of displacement. It could be in the form of strain or stress provided that the relationships are linear. Similarly, the input may be wind speed, acceleration, wave height, etc. and need not be force, but again the relationships must be linear.

To get the transfer function into the correct units for a PSD analysis the response parameter (per unit input loading) has to be squared. This is because the units of PSD's are units of interest squared, per hertz. If one takes the example of an offshore platform the input loading is typically expressed as a sea state spectrum. The process that this PSD defines is the sea surface elevation profile. In the time domain this is the sea surface elevation variation with time. The units of the input PSD, transfer function and response PSD are therefore given as:

Input PSD x transfer function = response PSD

$$\frac{m^2}{Hz} \quad x \quad \left[\frac{MPa}{m}\right]^2 \quad = \quad \frac{MPa^2}{Hz}$$

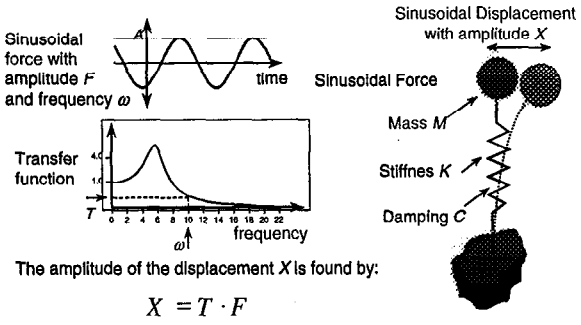

Figure 14. The concept of a linear transfer function

4. A PRACTICAL GUIDE TO USING THE FFT

There are a number of important issues to remember when using the FFT on real data. For example, the FFT algorithm is only suitable for time signals with 2^m data points, i.e.. 32, 64, 128, 256, ... data points. In this section a number of other practical issues pertaining to successful frequency domain analysis are discussed.

The Nyquist frequency

The maximum frequency calculated by the PSD is governed by a theoretical limit known as the ***Nyquist Frequency***. This is defined as half the sampling frequency used in the data analysis. When choosing a sample rate for data acquisition it is therefore necessary to set a value of at least twice that of the maximum frequency content of the process being recorded.

sample frequency = 2 x f_φ (5)

Frequency resolution

The Nyquist frequency and the number of points in the time sample govern the frequency resolution (δf). The interval between each calculated frequency is given by (see Figure 15):

$\delta f = f_\varphi$ / number of points in sample (6)

Frequency resolution is therefore improved as the sample length is increased.

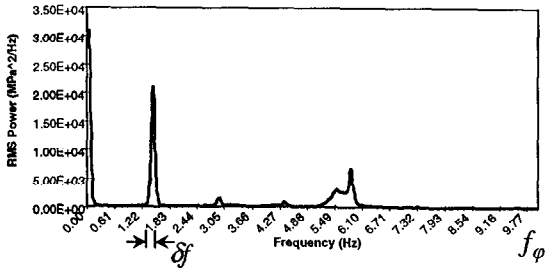

Figure 15. ∂f and Nyquist frequency

Aliasing

One of the biggest problems associated with acquiring data is that of aliasing. If data is sampled which contains sine waves with a frequency greater than the Nyquist frequency then the FFT algorithm will misinterpret the frequency of these sine waves. In order to see this it is worth sampling (draw dots on by hand) a sine wave just above and just below twice the Nyquist frequency. It will be seen that the sampling rate higher than twice the Nyquist rate correctly interprets frequency. However, it will be seen that the lower sampling rate predicts inaccurate frequencies. To avoid this it is customary to use anti aliasing (low pass) filters set somewhere below the Nyquist frequency.

The use of buffers and buffer averaging

It was mentioned earlier that the FFT algorithm was limited to calculating time histories with only 2^m data points (where m is an integer greater than 2.) In practice data is seldom acquired with exactly this number of points and so we need a method of subdividing the data into smaller 'buffers', each containing the required number of points. This is also done for reasons of computational efficiency and because statistical scatter reduces with increasing numbers of buffers.

We can therefore run the FFT algorithm for each buffer in turn to obtain a PSD for each (see Figure 16). The average PSD of the whole time history is then calculated by taking the linear average of all the buffers.

It is quite common for the time history to be too short to completely fill the last buffer; in this case the buffer can be padded with zeros at the end of the time history in order to fill it with the required number of data points.

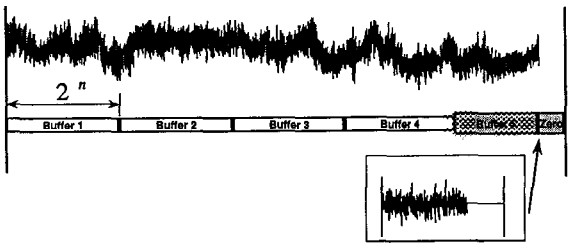

Figure 16. The use of buffers to compute the PSD

The Use of Windowing Functions

A potential problem arises when we calculate the PSD for a discrete buffer. To explain this problem consider the simple case of a single sine wave of frequency 6Hz (see Figure 17). Now if we take a buffer of 1 second, we can see that 6 complete sine cycles are included in the buffer. A PSD calculation of this results in a single spike centred at 6Hz.

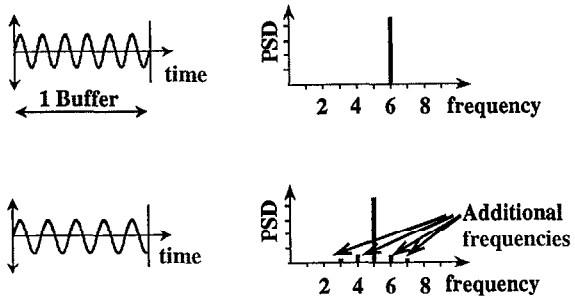

Figure 17. Spectral leakage

Suppose we now carry out the same analysis on a sine wave with frequency 4.8Hz. Now, the FFT assumes that this window, with 4.8 cycles, is joined to an identical one before and afterwards. This introduces a step in the continuous function. This then introduces additional frequencies, which are described using the term ***spectral leakage.***

To overcome the problem of discontinuous steps in the periodic time history we can choose to use a smoothing function, such as the Hanning window. This multiplies the start and end of the buffer by zero and gradually increases until reaching a maximum at the centre (see Figure 18). Such a smoothing function eliminates any large steps in the periodic time history and can improve the frequency result. However, some bias is also introduced into the process so the appropriate solution is not always clear.

There are many different windowing functions available, the choice of which one to use is down to the individual, some are better than others. A rectangular window uses the time signal without alteration.

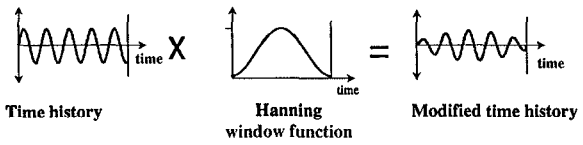

Figure 18. An example of window types (Hanning)

5. FATIGUE LIFE ESTIMATION FROM PSD'S

Before introducing the concepts needed to estimate fatigue damage in the frequency domain it is useful to set out a parallel approach in the time domain. The approach highlighted is that of a traditional S-N (Stress-Life) approach (see Figure 19).

Time Domain S-N Fatigue Life Estimation

The starting point for any fatigue analysis is the response of the structure or component, which is usually expressed as a stress or strain time history. If the response time history was made up of constant amplitude stress or strain cycles then the fatigue design could be accomplished by referring to a typical S-N diagram. However, because real signals rarely conform to this ideal constant amplitude situation, an empirical approach is used for calculating the damage caused by stress signals of variable amplitude.

Despite its limitations, the Palmgren-Miner rule is generally used for this purpose. This linear relationship assumes that the damage caused by parts of a stress signal with a particular range can be calculated and accumulated to the total damage separately from that caused by other ranges. A ratio is calculated for each stress range, equal to the number of actual cycles at a particular stress range, *n*, divided by the allowable number of cycles to failure at that stress, *N*, (obtained from the S-N curve). Failure is assumed to occur when the sum of these ratios, for all stress ranges, equals 1.0.

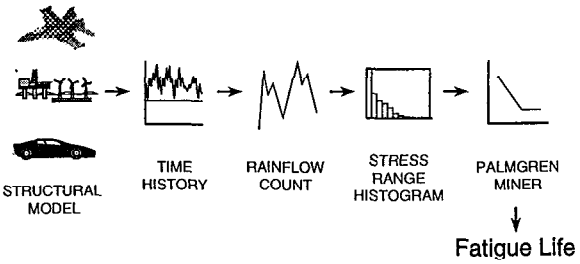

Figure 19. A standard S-N fatigue analysis

If the response time history is irregular with time, as shown in the Figure 19, then ***rainflow*** cycle counting is widely used to decompose the irregular time history into equivalent sets of block loading. The numbers of cycles in each block are usually recorded in a stress range histogram. This can then be used in the Palmgren Miner calculation. An example of the way rainflow ranges are extracted from a time signal is given in [3].

S-N Relationship

A traditional S-N curve as shown in Figure 20 is used to model the material properties of the components being analyzed. This simply shows that, under constant amplitude cyclic loading, a linear relationship exists between cycles to failure N and applied stress range S when plotted on log-log paper. There are two alternative ways of defining this relationship, as given below.

$$NS^m = K \qquad N^{-b}S = SRI1 \qquad (7)$$

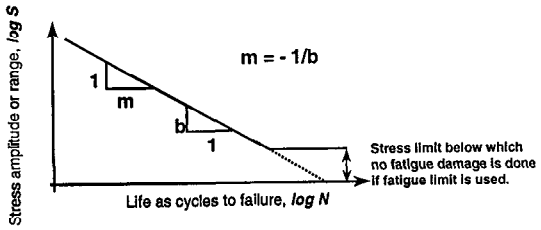

Figure 20. A typical S-N curve

Estimating fatigue life from a stress pdf

Once the stress range histogram has been converted into a stress range pdf then there is an elegant and efficient equation to describe the expected fatigue damage caused by this loading history.

$$E[D] = E[P]\frac{T}{k}\int_0^\infty S^m p(S)dS \qquad (8)$$

In order to compute fatigue damage over the lifetime of the structure in seconds (T) the form of material (S-N) data must also be defined using the parameters k and m (or b and $SRI1$). In addition, the total number of cycles in time T must be determined from the number of peaks per second E[P]. If the damage caused in time T is greater than 1.0 then the structure is assumed to have failed. Or alternatively the fatigue life can be obtained by setting T = 1.0 and then finding the fatigue life in seconds from equation 8:

The Frequency Domain Model

Figure 19 highlighted the overall process for fatigue life estimation in the time domain. The parallel approach in the frequency domain is shown in Figure 21. If we assume that the structural model shown is now an FEA model, this model would be identical for both the time domain and frequency domain approaches.

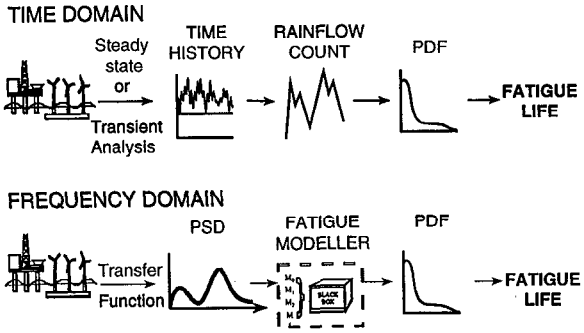

Figure 21. Time versus frequency domain calculations

In order to get structural response in the time domain a transient structural analysis would be required, before the fatigue analysis. In the frequency domain a transfer function would first be computed for the structural model. This is completely independent of the input loading and is a fundamental characteristic of the system, or model. The PSD response, caused by any PSD of input loading, is then obtained by multiplying the transfer function by the input loading PSD. Further response PSD's caused by additional PSD's of input loading can then be calculated with a trivial amount of computing time. Once the response PSD has been computed the remaining task is to estimate the fatigue damage using one of a number of fatigue models.

Narrow band solution

JS Bendat [11] presented the theoretical basis for the first of these of these frequency domain fatigue models, the so-called ***Narrow Band*** solution. This expression was defined solely in terms of the spectral moments up to m_4. However, the fact that this solution was suitable only for a specific class of response conditions was an unhelpful limitation for the practical engineer. The narrow band formula is given below.

$$E[D] = \sum_i \frac{n_i}{N(S_i)} = \frac{S_t}{k}\int S^b.p(S)\ dS$$

$$= \frac{E[P].T}{k}\int S^b.\left[\frac{S}{4m_0}e^{\frac{-S^2}{8m_0}}\right]\ dS \qquad (9)$$

This was the first frequency domain method for predicting fatigue damage from PSD's and it assumes that the pdf of peaks is equal to the pdf of stress amplitudes. The narrow band solution was then obtained by substituting the Rayleigh pdf of peaks with the pdf of stress ranges. The full equation is obtained by noting that S_t is equal to $E[P].T$, where T is the life of the structure in seconds (see Figure 22).

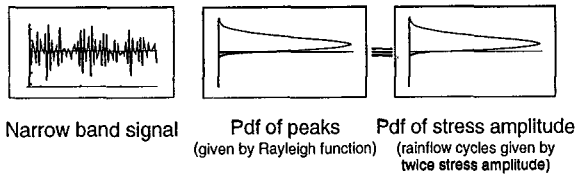

Figure 22. The basis of the narrow band solution

Figure 23 explains why the narrow band solution is so conservative for wide band cases? Two time histories are shown. The narrow band history (a) is made up by summing two independent sine waves at relatively close frequencies. The wide band history (b) uses two sine waves with relatively widely spaced frequencies.

Narrow banded time histories are characterised by frequency modulation known as a beat effect. Wide band processes are characterised by the presence of positive troughs and negative peaks and these are clearly seen in Figure 23 as a sinusoidal ripple superimposed on a larger, dominant sine wave.

The problem with the narrow band solution is that positive troughs and negative peaks are ignored, and all positive peaks are matched with corresponding troughs of similar magnitude regardless of whether they actually form stress cycles. To illustrate this, take every peak (and trough) and make a cycle with it by joining it to an imaginary trough (peak) at an equal distance the other side of the mean level. This is shown in Figure 23(c). It is easy to see that the resultant stress signal contains far more high stress range cycles than were present in the original signal. This is the reason why the narrow band solution is so conservative.

Empirical correction factors (Tunna, Wirsching, Hancock, Chaudhury and Dover)

Many expressions have been proposed to correct this conservatism. Most were developed with reference to offshore platform design where interest in the techniques has existed for many years. In general, they were produced by generating sample time histories from PSD's using Inverse Fourier Transform techniques. From these a conventional rainflow cycle count was then obtained.

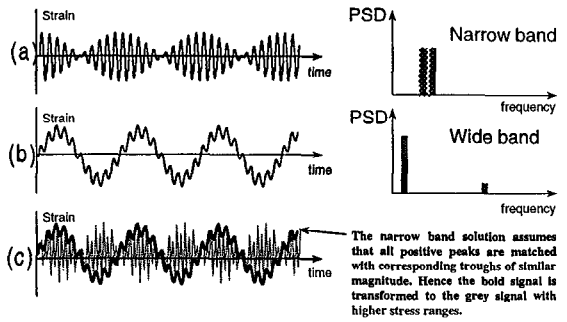

Figure 23. Why the narrow band solution is conservative

The solutions of **Wirsching** et al [12], **Chaudhury and Dover** [13], **Tunna** [3] and **Hancock** [14] were all derived using this approach. They are all expressed in terms of the spectral moments up to m_4.

Tunna

$$p(S)_T = \left[\frac{S}{4\gamma^2 \quad m_0} e^{-\frac{S^2}{8\gamma^2 m_0}} \right] \qquad (10)$$

Wirsching

$$E[D]_{Wirsch} = E[D]_{NB} \cdot \left[a(m) + [1 - a(m)](1 - \varepsilon)^{c(m)} \right]$$

where; a(m)=0.926-0.033m ; (11)
c(m)=1.587m-2.323 ;
$\varepsilon = \sqrt{1-\gamma^2}$

$$S_{eq} = \left[\int_0^\infty S^m p(S) dS \right]^{1/m}$$

Hancock equivalent stress

$$S_{eqHanc} = \left(2\sqrt{2m_0}\right) \left[\gamma \, \Gamma\left(\frac{m}{2} + 1\right) \right]^{1/m} \qquad (12)$$

Chaudhury & Dover equivalent stress

$$S_{eqC\&D} = \left(2\sqrt{2m_0}\right)\left[\frac{\varepsilon^{m+2}}{2\sqrt{\pi}}\Gamma\left(\frac{m+1}{2}\right)+\frac{\gamma}{2}\Gamma\left(\frac{m+2}{2}\right)+ erf(\gamma)\frac{\gamma}{2}\Gamma\left(\frac{m+2}{2}\right)\right]^{1/m} \quad (13)$$

where; $erf(\gamma) = 0.3012\gamma + 0.4916\gamma^2 + 0.9181\gamma^3 - 2.3534\gamma^4 - 3.3307\gamma^5 + 15.6524\gamma^6 - 10.7846\gamma^7$

Steinberg Solution

The approach of Steinberg leads to a very simple solution based on the assumption that no stress cycles occur with ranges greater than 6 rms values. The distribution of stress ranges is then arbitrarily specified to follow a Gaussian distribution. This defines the stress range cycles to occur with the following probability.

68.3% time at 2rms
27.1% time at 4rms
4.3% time at 6rms.

$$S_{eq\,Stein} = \left[0.683(\ 2\sqrt{m_0})^m + 0.271(\ 4\sqrt{m_0})^m + 0.043(6\ \sqrt{m_0})^m\right]^{1/m} \quad (14)$$

Dirlik's empirical solution for rainflow ranges

Dirlik [15] has produced an empirical closed form expression for the pdf of rainflow ranges, which was obtained using extensive computer simulations to model the signals using the Monte Carlo technique. Dirlik's solution is given below.

$$p(S) = \frac{\frac{D_1}{Q}e^{\frac{-Z}{Q}} + \frac{D_2 Z}{R^2}e^{\frac{-Z^2}{2R^2}} + D_3 Z e^{\frac{-Z^2}{2}}}{2(m_0)^{1/2}} \quad (15)$$

Where x_m, D_1, D_2, D_3, Q and R are all functions of m_0, m_1, m_2, and m_4 .Z is a normalised variable equal to $\frac{S}{2(m_0)^{1/2}}$.

Bishop's theoretical solution for rainflow ranges

Dirlik's empirical formula for the pdf of rainflow ranges has been shown to be far superior, in terms of accuracy, than the previously available correction factors. However, the need for certification of the technique before its use meant that theoretical verification was required. This was achieved by Bishop [4], when a theoretical solution for predicting rainflow ranges from the moments of the PSD was produced. A detailed description of this method is given in [5].

Most of the above techniques require an integration cut-off to be set in terms of the numbers of rms values along the stress range axis. It is normal to set this to 3 rms (for amplitude) or 6 rms (for range). However, it is easy to show, using measured signals of sufficient length, that up to 4.5 rms (on amplitude) is needed to avoid omitting fatigue-damaging cycles.

6. EXAMPLES

A simple hand calculation

In order to illustrate the mechanism of vibration fatigue calculations it is worth performing some simple hand calculations on the two-peaked PSD shown in Figure 24.

Approximate hand calculations have been performed in both the time and frequency domains. A computer-based calculation (using [16]) has also been performed as a comparison. This example is very useful for demonstrating that although the concepts underlying vibration fatigue tools may be complex it is still possible to use simple hand calculations to check results.

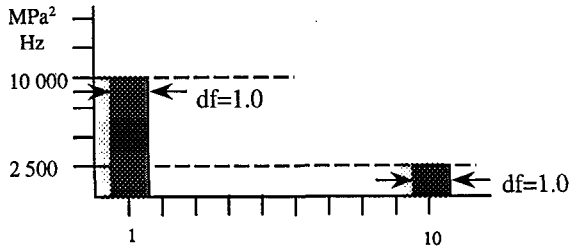

Figure 24. A simple 2 peaked PSD

Time domain by hand.

An approximate visualisation of the original time signal can be obtained by adding together two sine waves, one for each block in the PSD, where the amplitude of each is obtained (approximately) from 1.41 times the root mean square (rms) value (see Figure 25). Since the rms of each block can be calculated (approximately) from the square root of its area we get the following stress ranges:

- Sine wave 1 at 1Hz with a stress range of
  sqrt(10000) * 1.41 * 2 = 282 MPa
- Sine wave 2 at 10Hz with a stress range of
  sqrt(2500) x 1.41 x 2 = 141MPa

(N.B. Stress Range = 2 x Stress Amplitude)

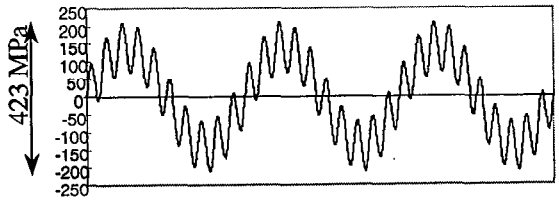

Figure 25. A time signal reconstructed from the 2 peaked PSD

If a rainflow counting procedure is adopted the 10Hz cycles are extracted, unaltered at 141MPa. This then leaves the 282MPa cycle compounded with the 141MPa cycle to create a rainflow cycle of range 423MPa. The rainflow count is therefore,

Table 2. Rainflow cycles counted from the simple time history

Number of cycles per Second	Total Rainflow Cycle Range
1	141MPa
10	423MPa

If we use a typical steel with S-N data of the form $N = 1.0E+15 * S^{-4.2}$ we get,

Table 3. Allowable N obtained from the S-N curve

Rainflow Cycle Range S	Cycles to Failure N
141MPa	**9.4E+5**
423MPa	**9.3E+3**

An approximate Palmgren-Miner damage calculation on the time signal then gives;

$$E[D] = \frac{10}{9.4E+5} + \frac{1}{9.3E+3} = 1.18E\text{-}4$$

This corresponds to a fatigue life of ***8462 secs***

Frequency domain by hand.

Moments can be computed easily from the PSD using the expression given earlier.

$m_0 = 12\,500$ $m_1 = 35\,000$

$m_2 = 260\,000$ $m_4 = 25\,010\,000$

From which we can compute

E[0] = 4.6 upward zero crossings per second and
E[P] = 9.8 peaks per second

$\gamma = 0.465$

rms = $\sqrt{m_0}$ = 112 MPa

From which we get an equivalent sine wave magnitude = 112 * 1.41 * 2 = 315 MPa.

For this, N(315MPa) = 3.2E+4

from which we can get a fatigue life of ***3265 secs***

Computer based calculations using MSC/FATIGUE.

Fatigue life using Narrow Band formula ***1472 secs***

Fatigue life using Dirlik ***7650 secs***

The correlation between the result obtained by hand (8462 seconds) and the Dirlik result (7650 seconds) is very good considering the simplifying assumptions that have been made. The hand calculation made with the narrow band assumption (3265 seconds) is also quite close to the computer based Narrow Band result (1472 seconds). As we would expect, the narrow band solution is conservative.

An FEA based example

In order to show the FEA based vibration fatigue approach a number of comparison calculations have been performed on the FEA model shown in Figure 26. This is a bracket, which is fully fixed at the position of the round hole.

Three loading time histories were applied at the end of the bracket in the horizontal, vertical, and twist directions.

Three frequency response results (in the range 0-50Hz) were obtained with unit forces and moments corresponding to the three load application points. These analyses were done in MSC/NASTRAN. The frequency response analyses used a damping ratio of 5% of critical. As an example Figure 27 shows the vertical frequency response result for one frequency of loading.

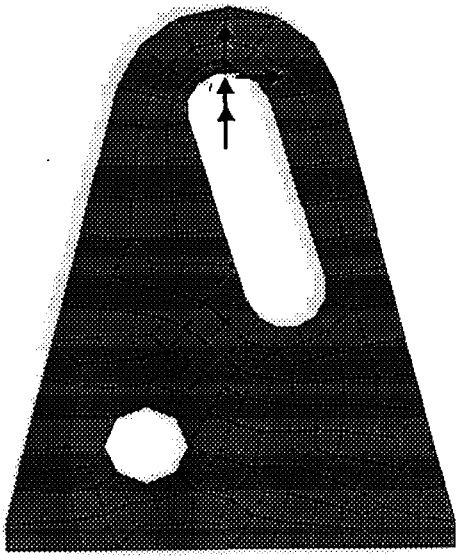

Figure 26. An FEA model of a simple bracket

Figure 28, Figure 29, and Figure 30 show the applied time histories, PSD's, and cross PSD's respectively. The cross PSD functions quite clearly show some correlation between load input signals.

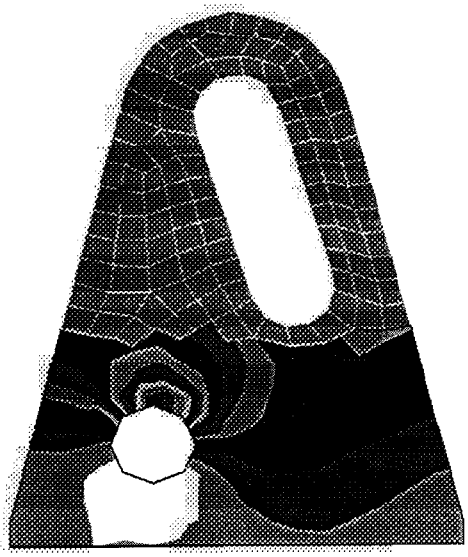

Figure 27. Frequency response results for a vertical load at zero hertz

Two separate comparisons have been made. Firstly, a static analysis comparison has been undertaken between the results from a conventional pseudo static analysis and the results from a PSD based analysis. With the pseudo static approach the results caused by each load application point are linearly superimposed at each node of interest. For both methods principal stresses were used.

In order to properly simulate a static situation the mass of the bracket was set sufficiently low to ensure that the first natural frequency was well above the maximum loading frequency. The first natural frequency was approximately 60Hz, with the highest frequency of loading being approximately 50Hz. Figure 31 and Figure 32 show good agreement between the two approaches for fatigue life. The red area (in this case dark grey near the circular hole) shows the position of the shortest life and the white areas (2 corners away from the hole) the longest fatigue lives.

The PSD and time history results for the most critical node are given in Figure 33 and Figure 34. The full set of comparison results for this node is given in Table 4.

Table 4. Time and PSD fatigue results for static model

Static model results in seconds		
	Static	**PSD Vibration**
Vertical	6.6E5	2.5E6
Horizontal	9.3E8	3.2E9
Twist	1.0E9	9.3E7
All together	4.0E4	5.1E3

The second comparison analysis was undertaken using a dynamic example. The same FE model was used but this time the mass was set so that several modes occurred in the loading frequency range. Mode 1 was at approximately 6Hz. Figure 35 shows mode 6, which occurred at 46Hz.

For this comparison a transient dynamic analysis was undertaken using MSC/NASTRAN. The stress output from this analysis was then analysed using MSC/FATIGUE. Figure 36and Figure 37 show the output from a critical node and Figure 38 and Figure 39 show the fatigue life contour plots for all nodes. Again, there is excellent agreement between the two approaches. As before, the red area (dark grey in this plot) shows the position of the shortest life and the white areas the longest fatigue lives. The full set of comparison results for this node is given in Table 5.

Table 5. Transient and PSD results for dynamic model

Dynamic model results in seconds		
	Dynamic	**PSD Vibration**
Vertical	145	38
Horizontal	1.9E9	9.8E8
Twist	3.7E7	3.8E5
All together	0.7	0.5

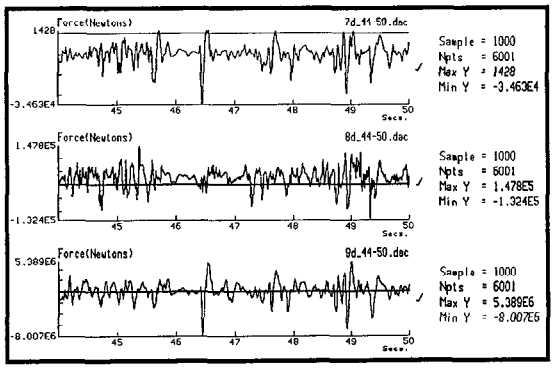

Figure 28. The 3 loading time signals

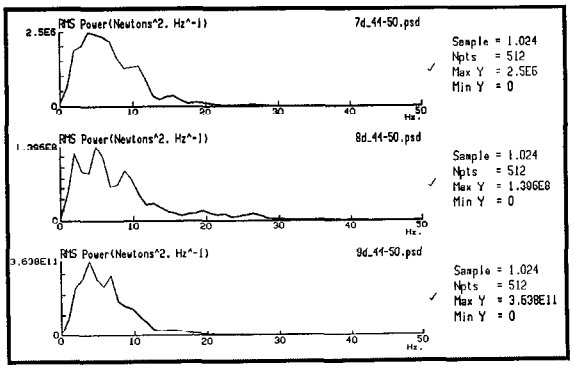

Figure 29. The 3 loading PSD's

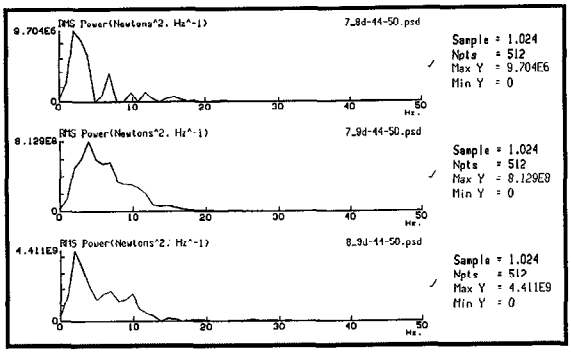

Figure 30. The 3 loading Cross PSD's

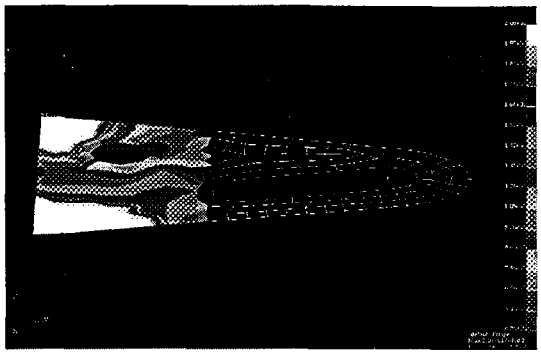

Figure 31. fatigue life for combined inputs from pseudo static analysis - static model

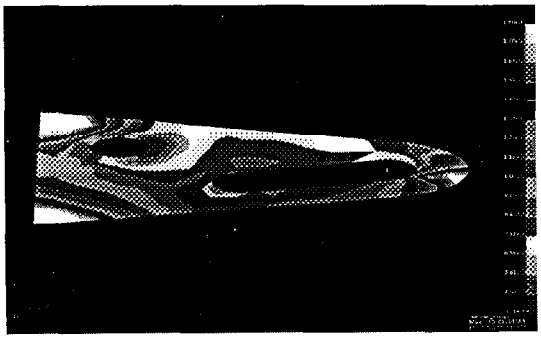

Figure 32. Fatigue life for combined inputs from PSD analysis - static model

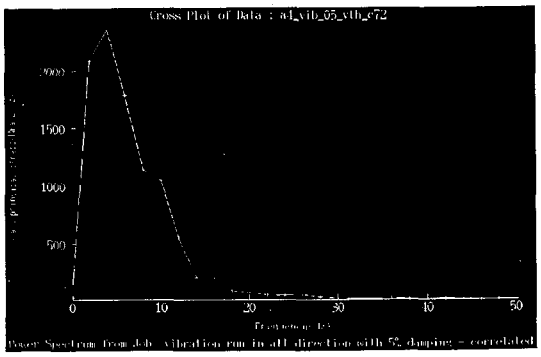

Figure 33. Output from critical node - PSD analysis, static model

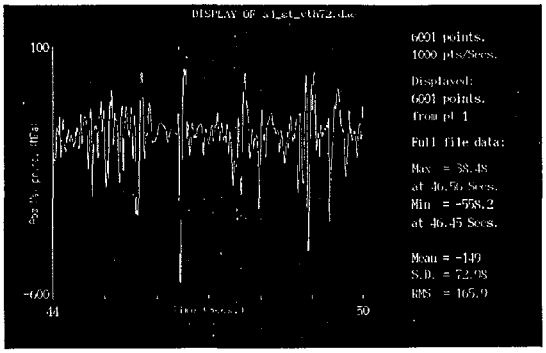

Figure 34. Output from critical node - pseudo static analysis, static model

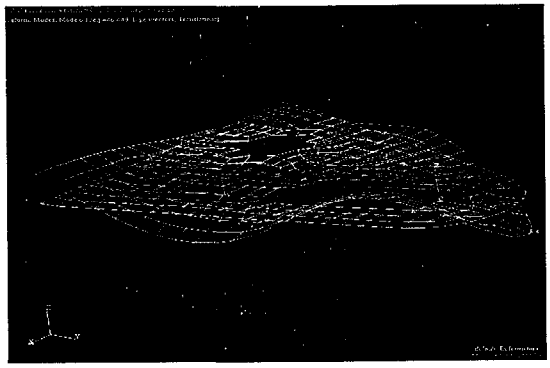

Figure 35. Mode 6 at 46 Hz

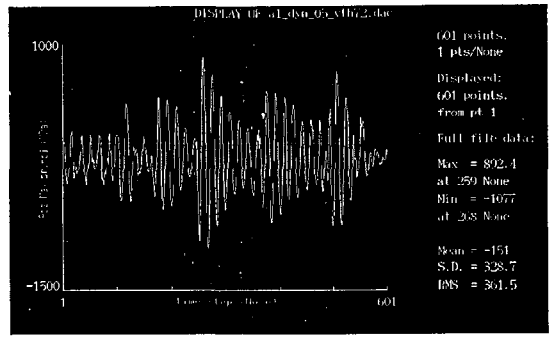

Figure 36. Output from critical node - transient analysis, dynamic model

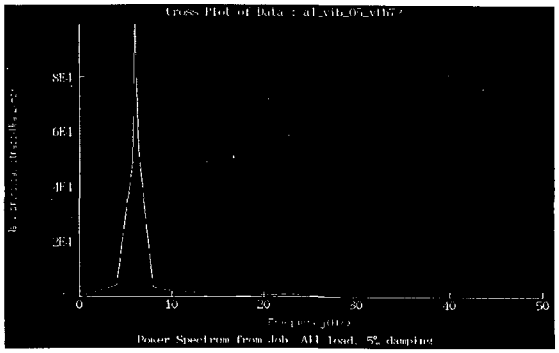

Figure 37. Output from critical node - PSD analysis, dynamic model

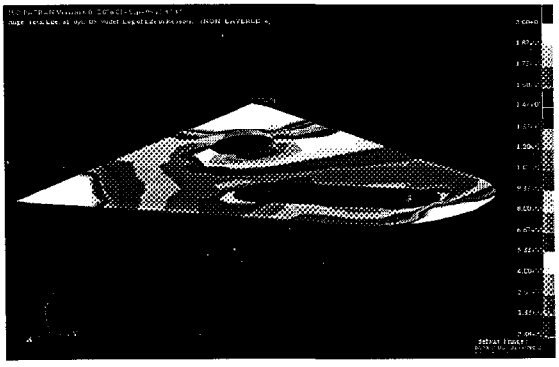

Figure 38. Fatigue life for combined inputs from transient analysis - dynamic model

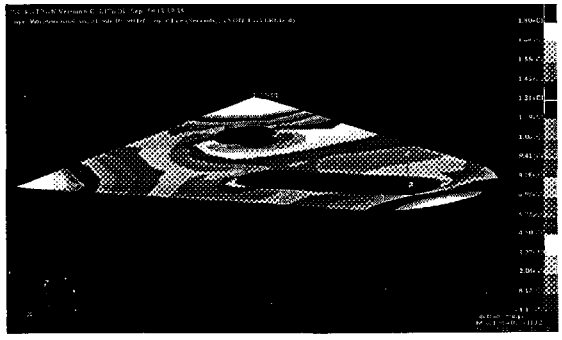

Figure 39. Fatigue life for combined inputs from PSD analysis - dynamic model

7. CONCLUSIONS

A state of the art review of vibration fatigue techniques has been presented. Although the underlying techniques are highly complicated it has been shown that a practical understanding of the techniques is sufficient to allow designers to usefully use these new tools. Several examples have been presented to show how the tools can be practically used for fatigue design, especially in the FEA environment.

8. REFERENCES.

[1] MSC/FATIGUE V8 User Manual, MSC Corporation, Los Angeles, CA, (1998).

[2] N W M Bishop, Dynamic fatigue response of deep water offshore structures subjected to random loading, Structural Engineering Review SER, **76/11**, 63-78, (1991).

[3] N W M Bishop and F Sherratt, Fatigue life prediction from power spectral density data. Part 1, traditional approaches and Part 2, recent developments. Environmental Engineering, **2**,(1989).

[4] N.W.M.Bishop, The use of frequency domain parameters to predict structural fatigue, PhD thesis, Warwick University, (1988).

[5] N.W.M.Bishop and F.Sherratt, A theoretical solution for the estimation of rainflow ranges from power spectral density data. Fat. Fract. Engng. Mater. Struct., **13**, 311-326, (1990).

[6] N.W.M.Bishop and F.Sherratt, Signal processing for fatigue in both the time and frequency domains, IMA Conference on Mathematics in the Automotive Industry, University of Warwick, 315-331, (1989).

[7] N W M Bishop, Z Hu, R Wang and D Quarton, Methods for the rapid evaluation of fatigue damage on the Howden HWP330 wind turbine, British Wind Energy Conference, York, (1993).

[8] N.W.M.Bishop , F Sherratt and Hu Zhihua, The Analysis of Non-Gaussian Loadings from Wind Turbine Blades Using Frequency Domain Techniques, British Wind Energy Conference 13, Swansea, 317-321, (1991).

[9] N.W.M.Bishop and Hu Zhihua, The Fatigue Analysis of Wind Turbine Blades Using Frequency Domain Techniques, European Wind Energy Conference, EWEC '91, Amsterdam, 246-250, (1991).

[10] Rice, SO. Mathematical analysis of random noise. Selected papers on noise and stochastic processes, Dover, New York, (1954).

[11] Bendat, JS. Probability functions for random responses. NASA report on contract NAS-5-4590, (1964).

[12] P.H.Wirsching and M.C.Light, Fatigue under wide band random loading, J Struct. Div., ASCE, 1593-1607, (1980).

[13] G.K.Chaudhury and W.D.Dover, Fatigue Analysis of Offshore Platforms Subject to Sea Wave Loading, Int J Fatigue, **7**, (1985).

[14] J.C.P.Kam and W.D.Dover, Fast fatigue assessment procedure for offshore structures under random stress history, Proc. Instn. Civ. Engrs., Part 2, **85**, 689-700, (1988).

[15] T.Dirlik, Application of computers in Fatigue Analysis, University of Warwick Thesis, (1985).

[16] MSC/FATIGUE V8 QuickStart Guide, MSC Corporation, Los Angeles, CA, (1998).